

Overpotential analysis of alkaline and acidic alcohol electrolyzers and optimized membrane-electrode assemblies

F. M. Sapountzi^{a*}, V. Di Palma^b, G. Zafeiropoulos^c, H. Penchev^d, M.A. Verheijen^b,
M. Creatore^b, F. Ublekov^d, V. Sinigersky^d, W.M. Arnold Bik^c, H.O.A. Fredriksson^a,
M.N. Tsampas^c, J.W. Niemantsverdriet^a

^a SynCat@DIFFER, Syngaschem BV, P.O. Box 6336, 5600 HH, Eindhoven, The Netherlands, www.syngaschem.com

^b Department of Applied Physics, Eindhoven University of Technology, 5600MB, Eindhoven, The Netherlands

^c DIFFER, Dutch Institute For Fundamental Energy Research, De Zaale 20, 5612 AJ, Eindhoven, The Netherlands

^d Institute of Polymers, Bulgarian Academy of Sciences, Acad. Georgi Bonchev 103A Str., BG 1113, Sofia, Bulgaria

*Corresponding author: Foteini Sapountzi, email: foteini@syngaschem.com, postal address: Syngaschem BV, P.O. Box 6336, 5600 HH, Eindhoven, The Netherlands

Abstract: Alcohol electrolysis using polymeric membrane electrolytes is a promising route for storing excess renewable energy in hydrogen, alternative to the thermodynamically limited water electrolysis. By properly choosing the ionic agent (i.e. H^+ or OH^-) and the catalyst support, and by tuning the catalyst structure, we developed membrane-electrode-assemblies which are suitable for cost-effective and efficient alcohol electrolysis. Novel porous electrodes were prepared by Atomic Layer Deposition (ALD) of Pt on a TiO_2 -Ti web of microfibers and were interfaced to polymeric membranes with either H^+ or OH^- conductivity. Our results suggest that alcohol electrolysis is more efficient using OH^- conducting membranes under appropriate operation conditions (high pH in anolyte solution). ALD enables better catalyst utilization while it appears that the TiO_2 -Ti substrate is an ideal alternative to the conventional carbon-based diffusion layers, due to its open structure. Overall, by using our developmental anodes instead of commercial porous electrodes, the performance of the alcohol electrolyser (normalized per mass of Pt) can be increased up to ~30 times.

34 **Keywords:** alcohol electrolysis; hydrogen production; porous electrodes; atomic layer
35 deposition; proton-conducting polymer; hydroxyl ion-conducting polymer

36

37 **1. Introduction**

38 Hydrogen is a potential energy carrier for storing excess power generated during the intermittent
39 operation of renewable energy sources. Among the different water electrolysis technologies^{1,2},
40 the use of polymeric exchange membranes (PEM) allows operation at low temperatures and
41 production of high purity hydrogen²⁻⁵. However, the efficiency of PEM electrolyzers is mainly
42 limited by the sluggish kinetics of the oxygen evolution reaction (OER)⁶. A promising approach
43 to deal with this issue is to replace OER by the electrooxidation of a sacrificial agent, which can
44 be an organic compound^{7,8}. For the specific case of using alcohols as the sacrificial agent, the
45 process is called alcohol electrolysis or electrochemical reforming of alcohols⁹. The power
46 demands for alcohol electrolysis can be significantly lower compared to conventional water
47 electrolysis. Table 1 gives indicatively the theoretical potentials and the half-reactions that take
48 place for the cases full oxidation of the alcohols to CO₂. Depending on numerous parameters
49 (chemical composition and structure of electrocatalyst, pH, electrolyte concentration etc), several
50 other reactions can take place leading to various intermediate products (CO, carbonates, acetic
51 acid, acetone etc)¹⁰⁻¹⁵.

52 The viability of the process has been discussed by Halme et al.¹⁶ in comparison to methanol fuel
53 cells and by Gutierrez-Guera et al.¹⁷ in comparison to the catalytic routes of alcohol reforming.
54 Finally, the electrolysis of water-alcohol solutions has potential for other applications, taking into
55 account that short-chain alcohols are present in industrial wastewater¹⁸. The feasibility of the
56 concept has been validated using several organic compounds^{9,19-49}. The aim of the present study
57 is to identify promising membrane-electrode-assemblies (MEAs) which can enable cost-effective
58 and efficient alcohol electrolysis.

59 Regarding the effect of the polymeric electrolyte, and thus the acidity/alkalinity of the anolyte
60 solution, we investigated the electrolysis of alcohol-water solutions using both H⁺ and OH⁻
61 conducting membranes. At the best of our knowledge, no comparison exists in literature between
62 alcohol-water electrolyzers operating with H⁺ and OH⁻ conducting membranes under identical

63 temperatures and alcohol concentrations and using the same electrode. The operation principle of
 64 the acidic (H^+) and alkaline (OH^-) PEM methanol-water electrolyzers is presented in Fig 1.

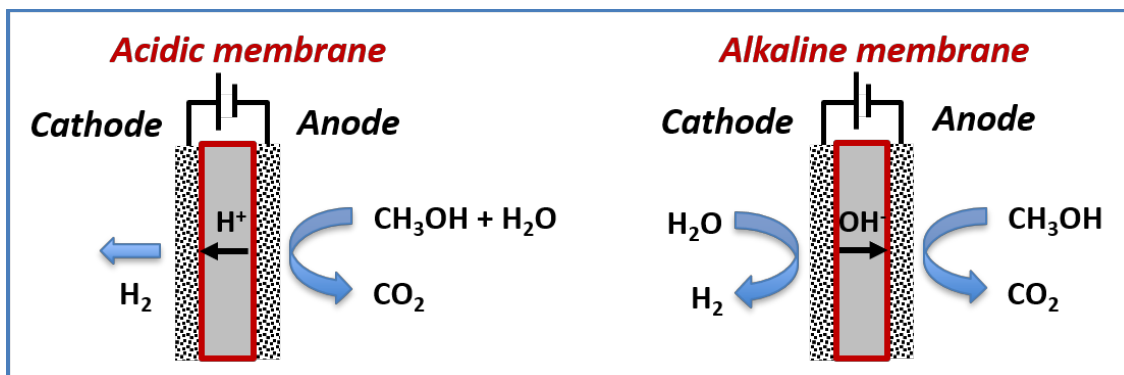
65

66 **Table 1.** Basic chemical reactions and theoretical potentials for different types of alcohol electrochemical reforming
 67 (Only the cases of full alcohol electrooxidation at the anode are given).

Alcohol	Electrochemical Reactions	Ionic agent	$E^0 = -\Delta G^0/nF$
Methanol	Anode: $CH_3OH + H_2O \rightarrow CO_2 + 6H^+ + 6e^-$ Cathode: $6H^+ + 6e^- \rightarrow 3H_2$ Total: $CH_3OH + H_2O \rightarrow CO_2 + 3H_2$	H^+	16 mV
	Anode: $6H_2O + 6e^- \rightarrow 6OH^- + 3H_2$ Cathode: $CH_3OH + 6OH^- \rightarrow CO_2 + 5H_2O + 6e^-$ Total: $CH_3OH + H_2O \rightarrow CO_2 + 3H_2$	OH^-	
Ethanol	Anode: $CH_3CH_2OH + 3H_2O \rightarrow 2CO_2 + 12H^+ + 12e^-$ Cathode: $12H^+ + 12e^- \rightarrow 6H_2$ Total: $CH_3CH_2OH + 3H_2O \rightarrow 2CO_2 + 6H_2$	H^+	84 mV
	Anode: $12H_2O + 12e^- \rightarrow 12OH^- + 6H_2$ Cathode: $CH_3CH_2OH + 12OH^- \rightarrow 2CO_2 + 9H_2O + 12e^-$ Total: $CH_3CH_2OH + 3H_2O \rightarrow 2CO_2 + 6H_2$	OH^-	
Propanol	Anode: $C_3H_7OH + 5H_2O \rightarrow 3CO_2 + 18H^+ + 18e^-$ Cathode: $18H^+ + 18e^- \rightarrow 9H_2$ Total: $C_3H_7OH + 5H_2O \rightarrow 3CO_2 + 9H_2$	H^+	106 mV for 2-propanol
	Anode: $18H_2O + 18e^- \rightarrow 18OH^- + 9H_2$ Cathode: $C_3H_7OH + 18OH^- \rightarrow 3CO_2 + 13H_2O + 18e^-$ Total: $C_3H_7OH + 5H_2O \rightarrow 3CO_2 + 9H_2$	OH^-	

68

69



70

71 **Figure 1.** Operation of PEM cells during electrolysis of methanol-water solutions using polymeric membranes
 72 with H^+ or OH^- conductivity as the electrolyte.

73

74 To optimize the electrode design and address the issue of catalyst utilization, electrodes were
 75 developed via Atomic Layer Deposition (ALD) of Pt on a porous TiO_2 -Ti substrate. For
 76 comparison reasons, identical experiments were carried out also using conventional Pt/C on
 77 carbon cloth electrodes. ALD is a thin-film deposition technique which has recently attracted
 78 much attention for the fabrication of electrocatalysts. ALD offers uniform dispersion of size-
 79 controllable catalyst nanoparticles over the entire surface of 3D substrates⁵⁰⁻⁵².

80 Overall, our results suggest that alcohol electrolysis can be more efficient using OH^- conducting
 81 membranes under appropriate operation conditions (high pH in anolyte solution). Moreover, we
 82 found that the implementation of the ALD process for the electrode preparation and of
 83 alternative TiO_2 /Ti substrates results in up to ~30 times more efficient catalyst utilization
 84 compared to commercial electrodes (Pt on carbon cloth).

85

86 **2. Experimental section**

87 **2.1 Polymeric membrane with H^+ conductivity**

88 A NafionTM 117 membrane with thickness 0.007 inch (Sigma Aldrich) was used as the proton-
 89 conducting electrolyte. Prior to its use, the membrane was treated by successive immersion in 15
 90 wt% H_2O_2 , 1 M H_2SO_4 and deionized H_2O at 80°C, 2 h for each step. Between each treatment
 91 step, the membrane was rinsed thoroughly with deionized H_2O .

92

93 **2.2 Polymeric membrane with OH⁻ conductivity**

94 A potassium hydroxide doped para-PBI membrane was used as the hydroxyl ion (OH⁻)
95 conducting electrolyte and was prepared by following a recently published procedure⁵³. In short,
96 in order to achieve high doping level of KOH electrolyte, we started from highly phosphoric acid
97 doped sol-gel p-PBI membrane, which after acid washing and neutralization is subsequently re-
98 doped with 50 wt% KOH solution. This affordable method allows much higher degree of alkali
99 doping (and thus much higher OH⁻ conductivity) than the traditionally applied imbibing method,
100 where dry PBI is immersed in lower concentration KOH solutions, usually at high temperatures
101 for a prolonged time.

102

103 **2.3 Porous electrode preparation**

104 The geometric surface area of anode and cathode was 3.1 cm². Commercial 1 mg/cm² Pt (20%
105 Pt/C) on carbon cloth was used for the cathode during all experiments. Two different kinds of
106 porous electrodes served as the anode of the cell: commercial electrodes with 1 mg/cm² Pt (20%
107 Pt/C) loaded on carbon cloth (ElectroChem Inc.) and electrodes fabricated via Atomic Layer
108 Deposition (ALD) of Pt on a porous TiO₂-Ti substrate (where TiO₂ represents the native oxide
109 surface). As described elsewhere⁵⁴, Ti-felts (Bekinit, 20 μm microfibers, 80% porosity) were
110 cleaned by sonication in acetone and in ethanol for 20 min, respectively and rinsed with
111 deionized water.

112 Pt was deposited on the porous TiO₂-Ti felt by 100 ALD cycles using a home-made deposition
113 system described in detail elsewhere⁵⁵. The base pressure of the reactor was <10⁻⁶ mbar.
114 MeCpPtMe₃ (98% from Sigma Aldrich) was used as precursor and O₂ gas at 1 mbar as reactant.
115 The precursor was contained in a stainless steel cylinder, heated at 30 °C, and brought into the
116 reactor using Ar as carrier gas. The lines from the precursor to the reactor were heated to 50 °C
117 and the reactor wall to 90 °C. The ALD recipe starts by dosing MeCpPtMe₃ for 4 s, then using 3
118 s of Ar to purge the precursor line, followed by 3 s of pumping down. Then O₂ gas is dosed for
119 10 s and afterwards the reactor is pumped down for 10 s. The deposition was carried out with the
120 substrate holder maintained at 300 °C.

121

122 *2.4 Characterization of Pt/TiO₂-Ti prepared by ALD*

123 The surface morphology of the Pt/TiO₂-Ti electrode was characterized with a scanning electron
124 microscope (FEI Quanta 3D FEG, at an acceleration voltage of 15 keV and working distance of
125 10 mm) and transmission electron microscope (JEOL ARM 200 probe corrected TEM, operated
126 at 200 kV, equipped with a 100 mm Centurio SDD EDS detector). The TEM sample was created
127 by peeling off individual fibers from the sample, and subsequently gluing them to a copper
128 support. The fibers themselves were far too thick to be electron transparent. In some thin edges
129 of the fibers, Pt particles could be imaged. Based on the open structure of the fiber network we
130 assumed that the images show a Pt distribution that is representative for the entire sample.

131 Rutherford Backscattering (RBS) analysis⁵⁶ was performed with a 2 MeV ⁴He beam delivered by
132 the 3.5 MV HVE Singletron installed at DIFFER (figure S1). In this particular case, the angle of
133 incidence could not be freely chosen and amounted to 41° with respect to the sample normal.
134 The particle detector was located at a scattering angle of 147°, resulting in an 8° exit angle of the
135 scattered particles with the sample normal. The combination of the non-perpendicular incidence
136 angle with the fiber-like texture of the samples gave rise to shadowing effects; a large fraction of
137 the incidence ions reached the sample ‘under’ fibers which blocked scattered particles on their
138 way to the detector. Fortunately, this fraction was equal for all samples and amounted to 37±3%.
139 The Pt loading is determined by simulation performed by WiNDF⁵⁷. For these simulations, 63%
140 of the actual charge has been used. The final Pt loading is estimated to be 0.025 mg/cm², which
141 has a similar order of magnitude to reported loadings after 100 Pt LD cycles on electrodes for
142 PEM fuel cells⁵⁸.

143

144 *2.5 Experimental setup and methods*

145 The experiments were carried out in a dual-chamber, separated electrochemical reactor made
146 from borosilicate glass (Pine Research Instrumentation, figure S2) as described elsewhere⁴⁴. The
147 catholyte chamber was filled with 0.3 M H₂SO₄ or 0.3 M KOH solution for the experiments with
148 H⁺ and OH⁻ conducting membranes respectively. The alcohols (methanol, ethanol, iso-propanol,
149 Sigma Aldrich, >99.5%) were introduced in the anolyte after mixing with proper amounts of

150 H₂SO₄ or KOH solutions. Between studies of different alcohols, the MEA was washed by
151 immersion in ultrapure water and dried in air at 70°C.

152 The experiments were carried out at room temperature. Polarization data were collected using an
153 Ivium Vertex potentiostat, equipped with an integrated impedance interface. The cell impedance
154 was measured using a frequency range from 10 kHz to 10 mHz with a potential amplitude of 10
155 mV. All overpotential values are calculated versus the potential at zero cell current.

156

157 **3. Results and discussion**

158 ***3.1. Acidic vs alkaline membranes***

159 Figure 2 gives a comparison of the potential losses when alcohol electrolysis is carried out with
160 H⁺ or OH⁻ conducting membranes. The total cell overpotential, η_{total} , is shown together with its
161 anodic (η_{an}), cathodic (η_{cath}) and ohmic (η_{ohm}) components. For the experiments of Figure 2, a
162 commercial anode of Pt/C on carbon cloth was used during the electrolysis of methanol, ethanol
163 and iso-propanol.

164

165

166

167

168

169

170

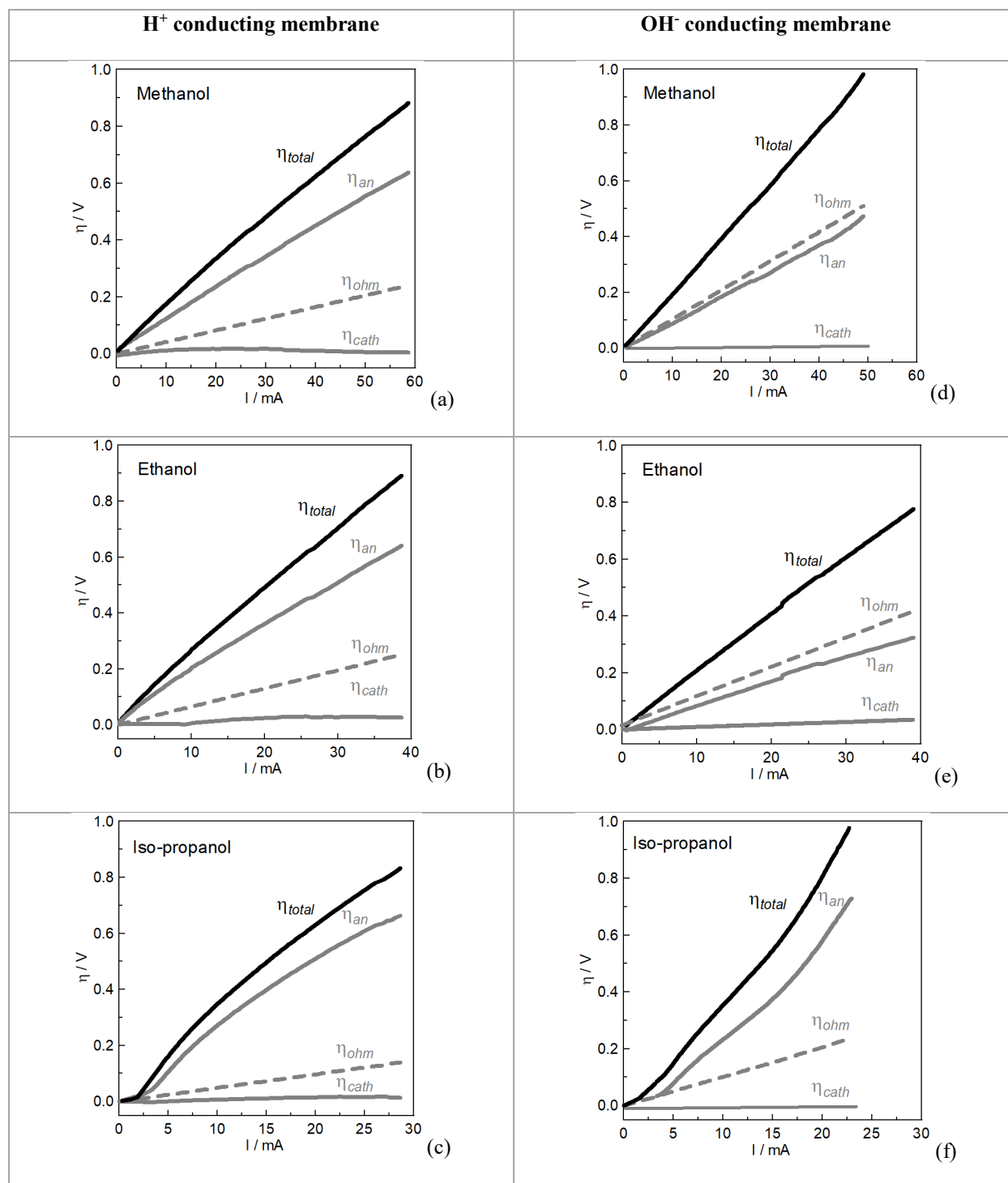
171

172

173

174

175



176 **Figure 2.** Effect of the cell current on the total cell overpotential and on the individual anodic, cathodic and ohmic
 177 overpotentials for (a,d) methanol, (b,e) ethanol, (c,f) iso-propanol. Figures a, b, c correspond to operation with H⁺
 178 conducting polymeric membrane (Nafion) and data are obtained by our previous study⁴⁴, Figures d, e, f correspond
 179 to operation with OH⁻ conducting polymeric membrane (KOH doped-PBI). Forward scans are presented. Sweep rate
 180 is 10 mV/s. Anolyte: 5.5 M alcohol + 0.2 M H₂SO₄ (a,b,c) or 0.2 M KOH (d,e,f).

181

182 As discussed in our previous study⁴⁴ for the case of H⁺ conducting electrolyte (Nafion),
183 overpotentials mainly originate from the slow anodic reaction (alcohol electrooxidation). In this
184 study we replaced Nafion by an OH⁻ conducting membrane (KOH doped PBI), and we observed
185 that the anodic losses become much lower for both methanol and ethanol electrolysis, while on
186 the other hand ohmic losses become larger. It is well-known that alkaline membranes cannot
187 reach the conductivity of Nafion⁵⁹. As a result, with the KOH doped-PBI membrane, anodic and
188 ohmic losses contribute almost equally to the total cell losses for the cases of methanol and
189 ethanol electrolysis. A small cathodic overpotential (~60 mV) was observed only during ethanol
190 electrolysis using the alkaline membrane. As discussed later, this observation is in line with EIS
191 measurements and can be attributed to extended ethanol crossover through the polymeric
192 membrane that causes the blocking of the cathodic active sites. The performance during
193 electrolysis of iso-propanol shows high anodic overpotentials at both acidic and alkaline
194 polymeric electrolytes, suggesting that iso-propanol electrolysis is not a viable technology under
195 the tested conditions. We assume that the high anodic overpotentials obtained with iso-propanol
196 are mainly related to the formation of strongly adsorbed intermediates⁴⁴⁻⁶⁰.

197 The beneficial role of the alkaline membranes towards the minimization of anodic losses is
198 clearly depicted in Table 2. The observed behaviour is in agreement with fundamental studies on
199 alcohol electrooxidation in aqueous media which have demonstrated an increased electrocatalytic
200 activity at alkaline pH⁶¹⁻⁶². Even though the use of OH⁻ conducting membranes seems a priori as
201 more promising for alcohol electrolysis due to the enhanced kinetics at high pH, the majority of
202 studies in the field utilize polymeric electrolytes with H⁺ conductivity. Tuomi et al.³¹ were the
203 first to carry out electrolysis of methanol-water solutions using an OH⁻ conducting polymeric
204 membrane. However, the obtained overall performance was inferior to previous studies with H⁺
205 conducting membranes, but it was unclear to the authors if this was related to the lower metal
206 loading used in their study or to the low ionic conductivity of the alkaline membrane. Our
207 analysis is performed using anodes with identical metal loadings and indicates that even though
208 electrocatalysis is favored at alkaline media (anodic overpotentials are lower, Table 2), the high
209 ohmic losses associated with the slow OH⁻ transport through the doped-PBI membrane have a
210 great impact on the overall performance of the electrolyser under the operational conditions of
211 the experiment of figure 2.

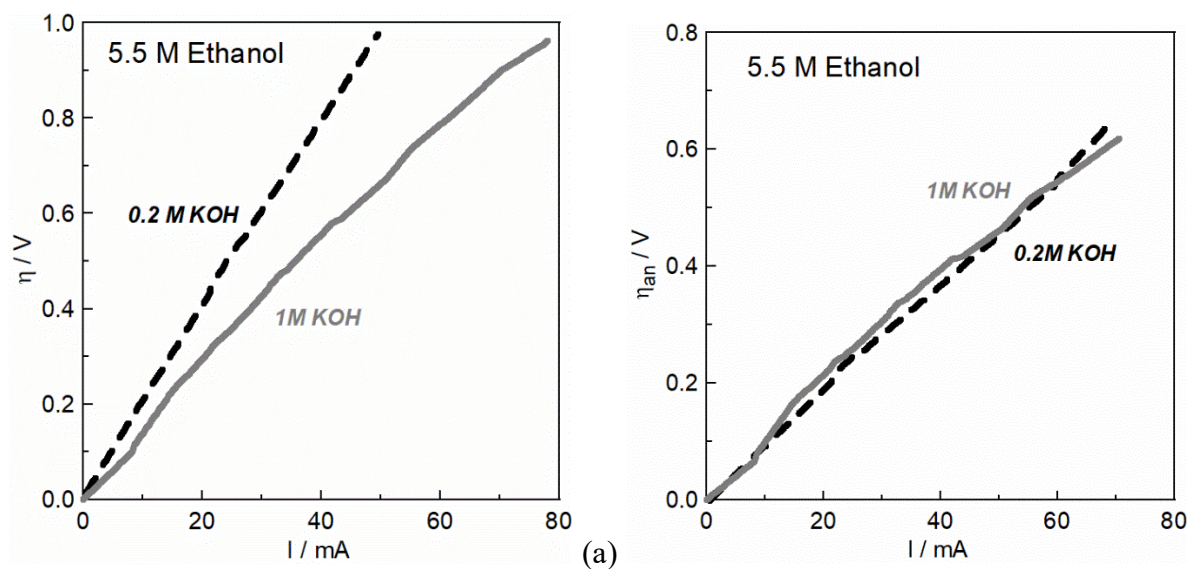
212 **Table 2.** Comparison of the current for different values of anodic overpotential, ionic agents and kinds of alcohol.
 213 Data for Nafion are obtained from literature⁴⁴.

Anodic overpotential	Current / mA					
	Methanol		Ethanol		Iso-propanol	
	H ⁺	OH ⁻	H ⁺	OH ⁻	H ⁺	OH ⁻
0.2 V	17.1	21.9	10.1	21.4	6.8	7.3
0.3 V	25.9	33.0	15.9	33.0	10.8	11.3
0.4 V	35.4	43.9	22.5	43.7	14.7	14.6

214
 215 However, the comparison between acidic and alkaline electrolyzers should be carried out
 216 carefully, since the operational parameters can greatly affect the performance. Specifically, the
 217 ionic conductivity of alkaline membranes is known to show high dependence on the KOH
 218 concentration⁶³⁻⁶⁷. On the other hand, it has been reported that the performance of ethanol
 219 electrolyzers with acidic membranes can be enhanced up to 20% upon properly adjusting the pH
 220 (by tuning the H₂SO₄ concentration in the anolyte feed), but this effect is only related to
 221 electrocatalytic properties of the anode since the ohmic resistance of Nafion remained unchanged
 222 upon pH variations in the acidic regime⁶⁸.

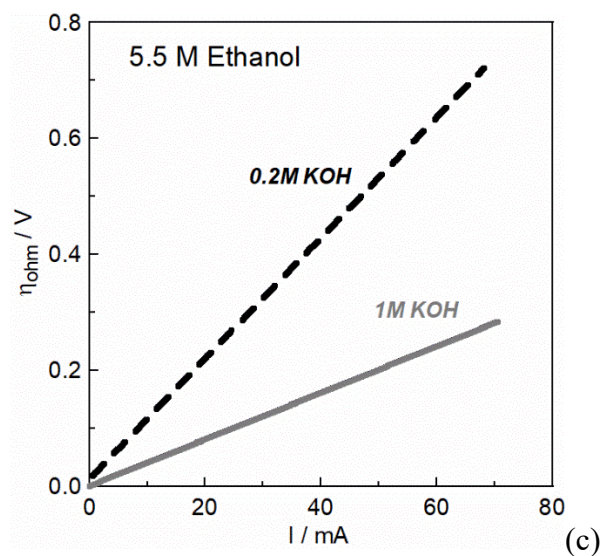
223 To allow a more fair comparison, we performed measurements with identical electrochemical
 224 cells operated with different KOH concentration in the anolyte solution. A ~70% increase in the
 225 overall cell performance was obtained by increasing the KOH concentration in the anolyte
 226 solution (figure 3a) by a factor of five. Deconvolution of the overpotential losses indicated that
 227 the improved overall performance under the more alkaline anolyte is only the result of enhanced
 228 ionic conductivity (figure 3c). The ohmic overpotential was the only type of overpotential
 229 affected by the changes in KOH concentration, as a result of higher ionic conductivity of the
 230 doped-PBI and also of the alcohol-KOH solution. As figure 3b shows, the anodic overpotential
 231 remains unchanged over the investigated current range upon alterations in the alkalinity of the
 232 anolyte solution, implying that electrocatalysis is not affected by the changes in KOH
 233 concentration from 0.2 M to 1.0 M. Overall, the results of figure 3 clearly indicate that under
 234 proper operation conditions, alcohol electrolyzers with alkaline membranes are more appropriate
 235 for practical applications, compared to those operated with acidic membranes.

236



237

238



239

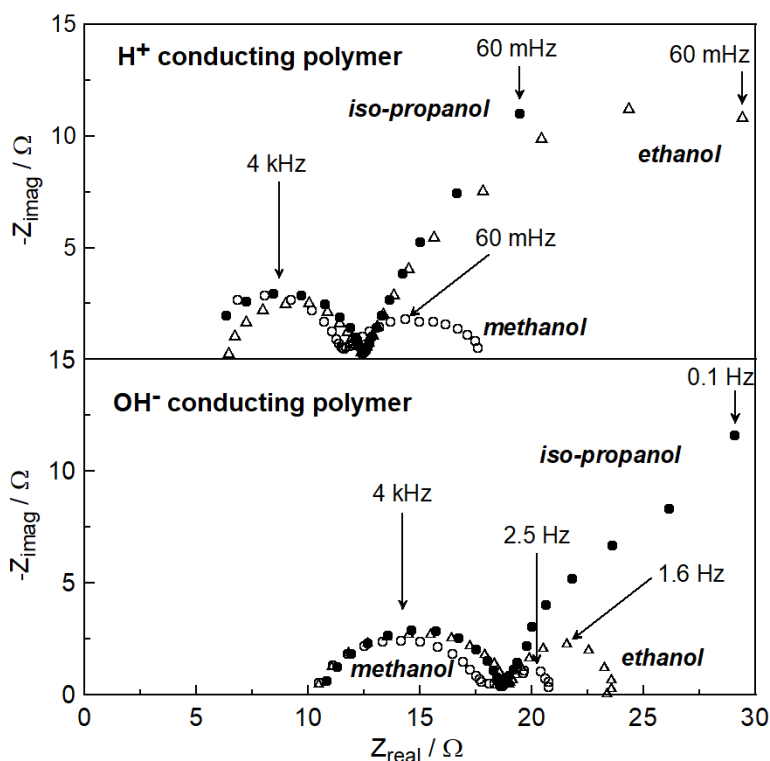
240 **Figure 3.** The dependence of current on total (a), anodic (b) and ohmic (c) overpotential using the doped-PBI
241 membrane during electrolysis of 5.5 M ethanol mixed with 0.2 M and 1.0 M KOH solutions. Sweep rate is 10 mV/s.

242

243 Electrochemical Impedance Spectroscopy (Figure 4) was used to further characterize the
244 electrolyzers. As discussed in our previous study⁴⁴, the ohmic resistance is affected by the
245 presence of alcohols for the case of Nafion-based cells (4.1, 6.5 and 5.0 Ω for methanol, ethanol
246 and iso-propanol respectively) indicating that interfacial phenomena take place and lead to ohmic

247 losses (changes in Nafion conductivity or membrane swelling). On the other hand, the ohmic
 248 losses remain unchanged for the case of doped-PBI (10.4 Ω), indicating that these interfacial
 249 phenomena are suppressed (the presence of alcohols causes less degree of swelling and/or
 250 negligible changes in the ionic conductivity of doped PBI membranes).

251 The low-frequency semicircle at the Nyquist plot is related to the anodic reaction since it is
 252 clearly affected by the kind of alcohol and the type of polymeric membrane. The high-frequency
 253 semicircle at the Nyquist plot is related to the cathodic hydrogen evolution reaction. Its width is
 254 related with the cathodic charge transfer resistance, which is independent of the nature of the
 255 alcohol for the case of Nafion, while it shows a small dependence on the alcohols for the case of
 256 KOH doped-PBI (7.8, 8.6 and 7.9 Ω for methanol, ethanol and iso-propanol respectively). The
 257 higher cathodic resistance (figure 4) and cathodic overpotential (figure 2e) observed only in
 258 presence of ethanol, provide evidence for extended ethanol crossover through the KOH doped-
 259 PBI membrane.



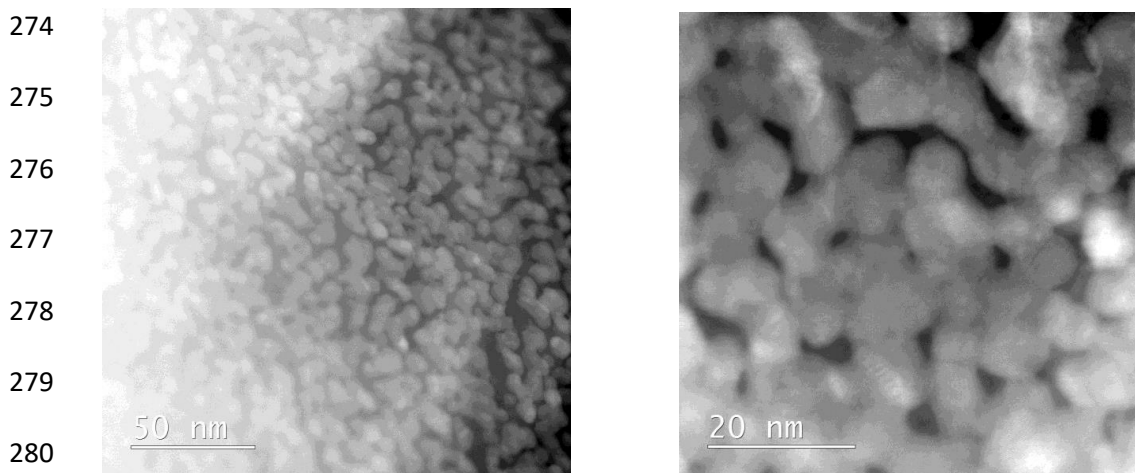
260
 261 **Figure 4.** Nyquist spectra at open-circuit conditions with different alcohols using Nafion (top) and doped-PBI
 262 (bottom) polymeric electrolytes. Anolyte: 5.5 M alcohol + 0.2 M H_2SO_4 or 0.2 M KOH. Data for Nafion adopted
 263 from reference 44.

264

265 **3.2. Novel porous electrodes**

266 As described in the experimental section, we explored a novel type of electrode by using ALD
267 for depositing Pt on a porous TiO₂-Ti substrate. TEM images of the Pt/TiO₂-Ti electrode are
268 shown in Figure 5. The presence and uniform distribution of the Pt particles can be clearly
269 discerned. Pt nanoparticles with an average size of 10 nm were obtained, but larger agglomerates
270 are also present.

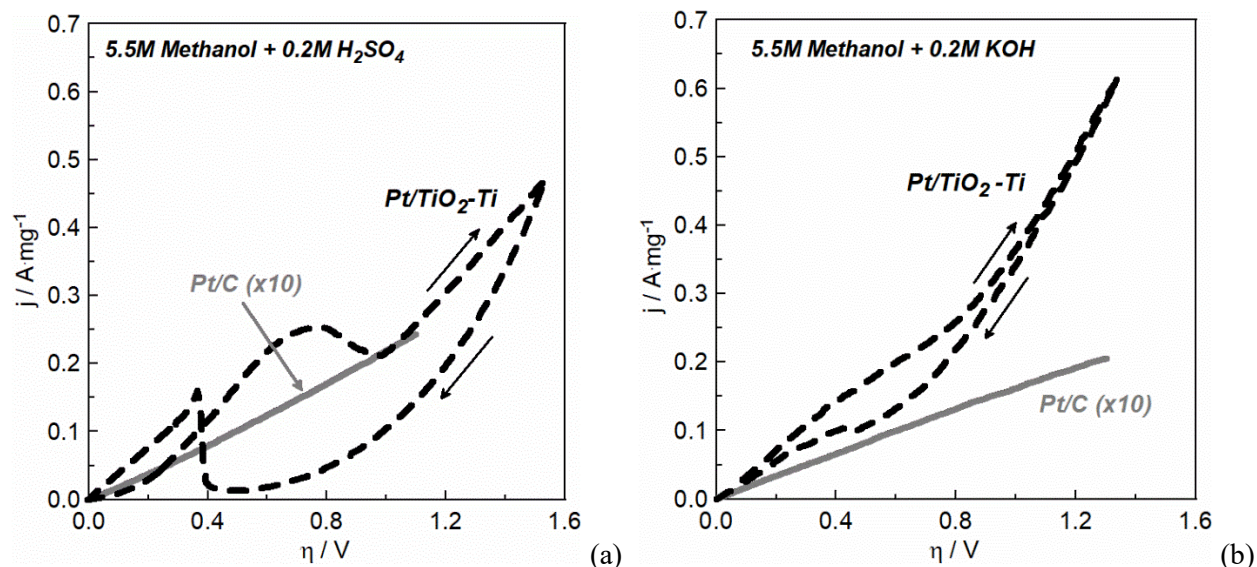
271 This electrode was interfaced to the one side of Nafion and KOH doped-PBI membranes and
272 served as the anode during methanol electrolysis in acidic and alkaline media, while using a
273 commercial Pt/carbon cloth cathode.



281 **Figure 5.** HAADF-STEM images displaying the Pt particle size on TiO₂-Ti substrate after 100 ALD
282 cycles.

283

284 Figure 6 shows the overall cell performance when using as the anode the novel Pt/TiO₂-Ti
285 electrode and the commercial Pt/C electrode. To enable comparison, per-mass normalized
286 currents (*j*) are presented in the polarization curves, while for better visualization *j* values are
287 multiplied by a factor of 10 for the case of commercial Pt/C anode. The Pt/TiO₂-Ti allowed for
288 up to 30 times higher Pt utilization compared to commercial electrodes when used with the
289 KOH-doped PBI membrane. When interfaced to Nafion membrane, the novel electrode shows up
290 to 10 times larger mass-normalized currents over the commercial electrode.



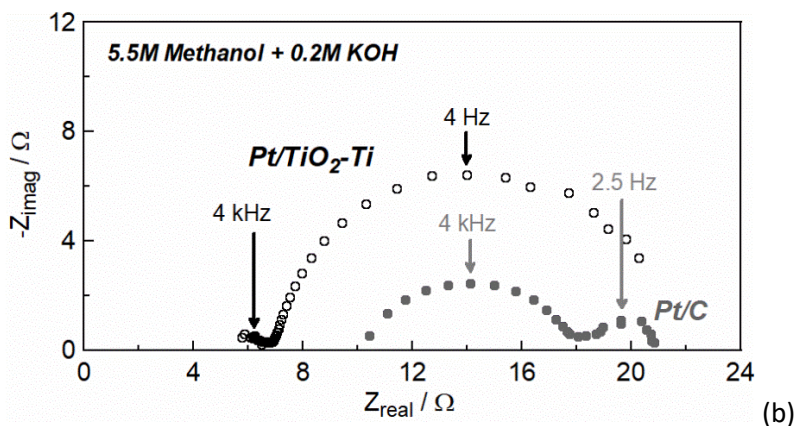
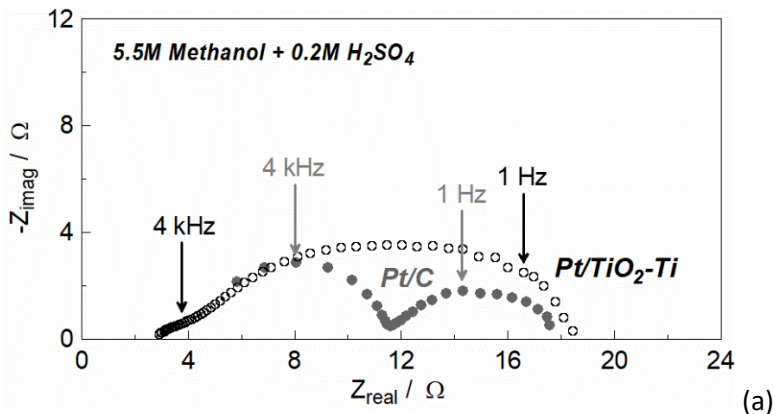
291
 292 **Figure 6.** Polarization curves during methanol electrolysis using the novel Pt(ALD)/TiO₂-Ti electrode and the
 293 commercial Pt/C carbon cloth electrode interfaced to (a) Nafion and (b) the doped-PBI membrane. Analyte: 5.5 M
 294 methanol mixed with (a) 0.2 M H₂SO₄ and (b) 0.2 M KOH solutions. Normalized current densities are 10 times
 295 multiplied for Pt/C. Sweep rate is 10 mV/s.

296
 297 Literature studies have reported 5-10 fold enhancement in the performance of PEM fuel cells and
 298 water electrolyzers upon depositing Pt by ALD on carbon-based diffusion layers, which is
 299 typically attributed to the uniform structural characteristics of Pt due to the deposition
 300 technique^{50,69}. We believe that in our case, the difference in performance is related to both the
 301 different Pt characteristics between the two anodes⁷⁰ (loading, particle size, particles geometry)
 302 and also to the open structure of the TiO₂-Ti substrate which facilitates the transport of reactants
 303 and products⁷¹⁻⁷². It has been observed in literature, that the use of TiO₂-based supports instead
 304 of C-based, can induce metal-support interactions which affect the electrocatalytic oxidation of
 305 alcohols⁷³⁻⁷⁴. However, it is not clear if these phenomena play a role also in our system.

306 Another interesting feature is the complexity of the voltammograms of figure 6. Forward and
 307 backward scans were identical with the Pt/C anode, while this is not the case for Pt/TiO₂-Ti. As
 308 shown in figure 6a, peaks in the voltammogram are observed due to the formation/oxidation of
 309 intermediate carbonaceous species. Using the doped-PBI, the hysteresis characteristics are
 310 suppressed and the voltammogram becomes less complex. This could be due to different reaction

311 mechanisms in acidic and alkaline media and to less accumulation of adsorbed intermediate
312 species.

313



316

317 **Figure 7.** Nyquist spectra during methanol electrolysis using the Pt/TiO₂-Ti electrode and the commercial Pt/C
318 carbon cloth electrode interfaced to (a) Nafion and (b) the KOH doped-PBI membrane. Anolyte: 5.5 M methanol
319 mixed with (a) 0.2 M H₂SO₄ and (b) 0.2 M KOH solutions.

320

321 Figure 7 presents the Nyquist plots during methanol electrolysis using the two different anodes
322 together with Nafion and the doped-PBI membrane. The semicircles in the Nyquist plots merge
323 when the novel anodes are used, indicating comparable time-constants of the anodic and cathodic
324 reactions. The ohmic resistance of the cell is lower for the cell with the Pt/TiO₂-Ti anode.
325 Specifically, the ohmic resistance with the Nafion-based cells is 2.9 Ω for Pt/TiO₂-Ti anode and
326 4.1 Ω for the Pt/C anode, while with the cells with the KOH doped-PBI electrolyte the ohmic
resistance is 6.9 Ω for Pt/TiO₂-Ti anode and 10.4 Ω for the Pt/C anode (figure 7). Based on the

327 resistance values and polarization data, Table 3 gives a detailed comparison of the actual
 328 performance of the electrolyzers in terms of current and ohmic and total overpotentials.

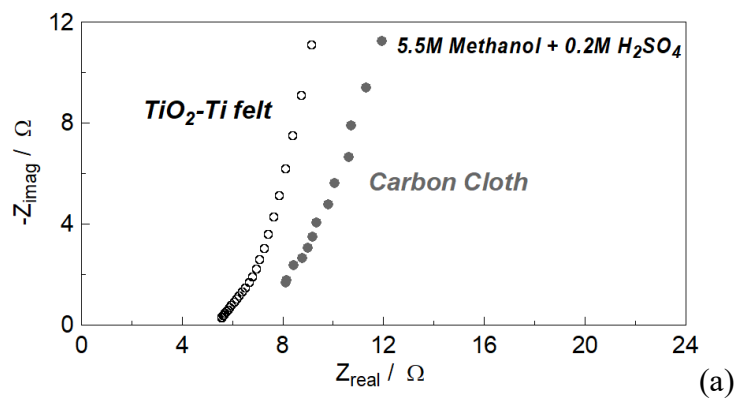
329

330 **Table 3.** Polarization data and overpotential values for acidic and alkaline methanol electrolysis with Pt/C and
 331 Pt/TiO₂-Ti anodes.

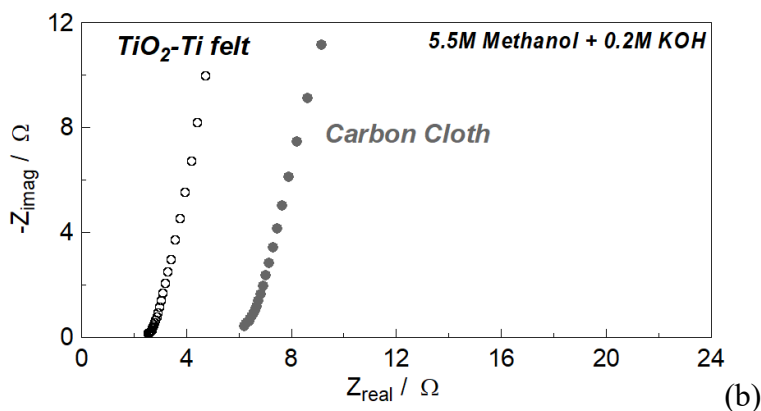
		Acidic				Alkaline			
		$\eta=1V$		$I= 35 \text{ mA}$		$\eta=1V$		$I= 35 \text{ mA}$	
<i>Anode</i>	<i>Pt-mass/ μg</i>	<i>I / mA</i>	<i>η_{ohm} / V</i>	<i>η/V</i>	<i>η_{ohm} / V</i>	<i>I / mA</i>	<i>η_{ohm} / V</i>	<i>η/V</i>	<i>η_{ohm} / V</i>
Pt/C	3100	62	0.25	0.56	0.15	47	0.49	0.69	0.36
Pt/TiO ₂ - Ti	77.5	16	0.05	1.50	0.10	29	0.20	1.14	0.24

332

333 EIS measurements using the plain substrates without any Pt loading also confirmed the lower
 334 resistance of the TiO₂-Ti substrate (figure 8). In our view, this difference can be attributed to the
 335 presence of a hydrophobic microporous layer on the carbon cloth, but not on the TiO₂-Ti
 336 substrate, and which can affect negatively the conductivity of gas diffusion substrates⁷⁵⁻⁷⁶.



337



338
 339 **Figure 8.** Nyquist spectra during methanol electrolysis using the plain TiO₂-Ti and carbon cloth
 340 substrates (no Pt loading) interfaced to (a) Nafion and (b) the doped-PBI membrane. Anolyte: 5.5 M
 341 methanol with (a) 0.2 M H₂SO₄ and (b) 0.2 M KOH solutions.

342
 343

344 **4. Conclusions**

345 Optimized membrane-electrode-assemblies were developed for the electrolysis of C1-C3
 346 alcohols, by properly selecting the kind of polymeric electrolyte and by designing optimized
 347 porous electrodes. In order to investigate the effect of the electrolyte, we carried out identical
 348 experiments of alcohol electrolysis with commercial electrodes using H⁺ and OH⁻ conducting
 349 polymeric membranes. The experiments were carried out under identical temperatures and
 350 alcohol concentrations and using the same electrode, while the pH of the anolyte solution was
 351 adjusted accordingly.

352 By deconvoluting the overpotential components, we found that the performance of both alkaline
 353 and acidic electrolyzers is limited by potential losses due to slow alcohol electrooxidation
 354 (anodic overpotential) and slow ion transfer (ohmic overpotential). Anodic overpotential is
 355 diminished when OH⁻ conducting polymers are used as the electrolyte (KOH-doped PBI), in
 356 agreement with literature studies using aqueous electrolyte solutions which report increased
 357 reaction rates in alkaline media. On the other hand, the ohmic losses in the OH⁻ conducting
 358 alcohol electrolyser are higher, due to the lower conductivity of these membranes compared to
 359 the H⁺ conducting Nafion. However, the conductivity of KOH-doped PBI membranes can be
 360 tuned by changing the pH of the anolyte solution. Overall, our results suggest that under

361 appropriate operation conditions (high pH), alkaline alcohol electrolysis can be more efficient
362 than acidic alcohol electrolysis, since both anodic and ohmic overpotentials are minimized.

363 The second goal of this study was to design novel anodes with enhanced catalyst utilization. For
364 this reason, Atomic layer Deposition of Pt was carried out on a porous TiO₂-Ti substrate and the
365 developmental anode was implemented in alkaline and acidic electrolyzers. Up to ~30 times
366 more efficient catalyst utilization was achieved compared to the commercial Pt on carbon cloth
367 anodes, as a result of optimized morphological electrode characteristics.

368

369 **Acknowledgements**

370 This project has received funding from the European Union's Horizon 2020 research and
371 innovation programme "CritCat" under grant agreement No 686053, from Synfuels China
372 Technology Co. Ltd (Beijing-Huairou, P.R. China) and from the Bulgarian Science Fund project
373 DFNI-E02/9. Solliance and the Dutch province of Noord-Brabant are acknowledged for funding
374 the TEM facility.

375

376

377

378 **References**

- 379 1. Chorkendorff I, Niemantsverdriet JW, Concepts of Modern Catalysis and Kinetics, 3rd Edition
380 Wiley-VCH, Weinheim; 2017. ISBN:978-3-527-33268-7
- 381 2. Sapountzi, F.M., Gracia JM, Fredriksson HOA, Weststrate CJ, Niemantsverdriet JW,
382 Electrocatalysts for the generation of hydrogen, oxygen and synthesis gas. Prog Energy Combust
383 Sci 2017; 58: 1-35. doi: 10.1016/j.pecs.2016.09.001
- 384 3. Carmo M, Fritz DL, Mergel J, Stolten D. A comprehensive review on PEM water electrolysis. Int
385 J Hydrogen Energy 2013;38:4901–34. doi:10.1016/j.ijhydene.2013.01.151.
- 386 4. Ferrero D, Lanzini A, Santarelli M, Leone P. A comparative assessment on hydrogen production
387 from low- and high-temperature electrolysis. Int J Hydrogen Energy 2013;38:3523–36.
388 doi:10.1016/j.ijhydene.2013.01.065.
- 389 5. Aricò AS, Siracusano S, Briguglio N, Baglio V, Di Blasi A, Antonucci V. Polymer electrolyte
390 membrane water electrolysis: Status of technologies and potential applications in combination
391 with renewable power sources. J Appl Electrochem 2013;43:107–18. doi:10.1007/s10800-012-
392 0490-5.

- 393 6. Acar C, Dincer I. Comparative assessment of hydrogen production methods from renewable and
394 non-renewable sources. *Int J Hydrogen Energy* 2014;39:1–12.
395 doi:10.1016/j.ijhydene.2013.10.060.
- 396 7. Coutanceau C, Baranton S. Electrochemical conversion of alcohols for hydrogen production: a
397 short overview. *Wiley Interdiscip Rev Energy Environ* 2016;5:388–400. doi:10.1002/wene.193.
- 398 8. Miller H, Vizza F, Fornasiero P, Co-production of hydrogen and chemicals by electrochemical
399 reforming of biomass-derived alcohols In: van de Voorde M, Sels B editors. *Nanotechnology in
400 Catalysis: Applications in the Chemical Industry, Energy Development and Environment
401 Protection*, Wiley-VCH Verlag GmbH&Co; 2017, doi: 10.1002/9783527699827.ch36
- 402 9. Ju HK, Giddey S, Badwal SPS, Mulder RJ. Electro-catalytic conversion of ethanol in solid
403 electrolyte cells for distributed hydrogen generation. *Electrochim Acta* 2016;212:744–57.
404 doi:10.1016/j.electacta.2016.07.062.
- 405 10. Altarawneh BM, Pickup PG. Product distributions and efficiencies for ethanol oxidation in a
406 proton exchange membrane electrolysis cell. *J. Electrochem. Soc.* 2017; 164: F861-865. doi:
407 10.1149/2.0051709jes.
- 408 11. Cantane DA, Ambrosio WF, Chatenet M, Lima FHB. Electro-oxidation of ethanol on Pt/C, Rh/C
409 and Pt/Rh/C-based electrocatalysts investigated by on-line DEMS. *J. Electroanal. Chem.* 2012;
410 681: 56-65. doi: 10.1016/j.jelechem.2012.05.024.
- 411 12. Wang H, Jusys Z, Behm RJ. Ethanol electrooxidation on a carbon-supported Pt catalyst: Reaction
412 kinetics and product yields. *J. Phys. Chem. B.* 2004; 108(50): 19413-19424. doi:
413 10.1021/jp046561k
- 414 13. Diaz V, Ohanian M, Zinola CF. Kinetics of methanol electrooxidation on Pt/C and PtRu/C
415 catalysts. *Int. J. Hydrogen Energy* 2010; 35(19): 10539-10546. doi:
416 10.1016/j.ijhydene.2010.07.135.
- 417 14. Tsiouvaras N, Martinez-Huerta MV, Paschos O, Stimming U, Gierro JLG, Pena MA. PtRuMo/C
418 catalysts for direct methanol fuel cells: Effect of the pretreatment on the structural characteristics
419 and methanol electrooxidation. *Int. J. Hydrogen Energy* 2010; 35(20): 11478-11488. doi:
420 10.1016/j.ijhydene.2010.06.053.
- 421 15. Perez-Rodriguez S, Corengia M, Garcia G, Zinola CF, Lazaro MJ, Pastor E. Gas diffusion
422 electrodes for methanol electrooxidation studied by a new DEMS configuration: Influence of the
423 diffusion layer. *Int. J. Hydrogen Energy* 2012; 37(8): 7141-7151. doi:
424 10.1016/j.ijhydene.2011.11.090.
- 425 16. Halme A, Selkänaho J, Noponen T, Kohonen A. An alternative concept for DMFC - Combined
426 electrolyzer and H₂ PEMFC. *Int J Hydrogen Energy* 2016;41:2154–64.
427 doi:10.1016/j.ijhydene.2015.12.007.
- 428 17. Gutiérrez-Guerra N, Jiménez-Vázquez M, Serrano-Ruiz JC, Valverde JL, de Lucas-Consuegra A.
429 Electrochemical reforming vs. catalytic reforming of ethanol: A process energy analysis for
430 hydrogen production. *Chem Eng Process Process Intensif* 2015;95:9–16.
431 doi:10.1016/j.cep.2015.05.008.

- 432 18. Majone M, Aulenta F, Dionisi D, D'Addario EN, Sbardellati R, Bolzonella D, et al. High-rate
433 anaerobic treatment of Fischer-Tropsch wastewater in a packed-bed biofilm reactor. *Water Res*
434 2010;44:2745–52. doi:10.1016/j.watres.2010.02.008.
- 435 19. Sasikumar G, Muthumeenal A, Pethaiah SS, Nachiappan N, Balaji R. Aqueous methanol
436 eletrolysis using proton conducting membrane for hydrogen production. *Int J Hydrogen Energy*
437 2008;33:5905–10. doi:10.1016/j.ijhydene.2008.07.013.
- 438 20. Take T, Tsurutani K, Umeda M. Hydrogen production by methanol-water solution electrolysis. *J*
439 *Power Sources* 2007;164:9–16. doi:10.1016/j.jpowsour.2006.10.011.
- 440 21. Pham AT, Baba T, Shudo T. Efficient hydrogen production from aqueous methanol in a PEM
441 electrolyzer with porous metal flow field: Influence of change in grain diameter and material of
442 porous metal flow field. *Int J Hydrogen Energy* 2013;38:9945–53.
443 doi:10.1016/j.ijhydene.2013.05.171.
- 444 22. Sethu SP, Ramalinga Viswanathan M, Mani U, Chan SH. Evaluation of impregnated
445 nanocomposite membranes for aqueous methanol electrochemical reforming. *Solid State Ionics*
446 2015;283:16–20. doi:10.1016/j.ssi.2015.11.006.
- 447 23. Cloutier CR, Wilkinson DP. Electrolytic production of hydrogen from aqueous acidic methanol
448 solutions. *Int J Hydrogen Energy* 2010;35:3967–84. doi:10.1016/j.ijhydene.2010.02.005.
- 449 24. Lamy C, Guenot B, Cretin M, Pourcelly G. (Invited) A Kinetics Analysis of Methanol Oxidation
450 under Electrolysis/Fuel Cell Working Conditions. *ECS Trans* 2015;66:1–12.
451 doi:10.1149/06629.0001ecst.
- 452 25. Guenot B, Cretin M, Lamy C. Clean hydrogen generation from the electrocatalytic oxidation of
453 methanol inside a proton exchange membrane electrolysis cell (PEMEC): effect of methanol
454 concentration and working temperature. *J Appl Electrochem* 2015;45:973–81.
455 doi:10.1007/s10800-015-0867-3.
- 456 26. Lamy C, Guenot B, Cretin M, Pourcelly G. Kinetics Analysis of the Electrocatalytic Oxidation of
457 Methanol inside a DMFC working as a PEM Electrolysis Cell (PEMEC) to generate Clean
458 Hydrogen. *Electrochim Acta* 2015;177:352–8. doi:10.1016/j.electacta.2015.02.069.
- 459 27. de la Osa AR, Calcerrada AB, Valverde JL, Baranova EA, de Lucas-Consuegra A.
460 Electrochemical reforming of alcohols on nanostructured platinum-tin catalyst-electrodes. *Appl*
461 *Catal B Environ* 2015;179:276–84. doi:10.1016/j.apcatb.2015.05.026.
- 462 28. Muthumeenal A, Pethaiah SS, Nagendran A. Investigation of SPES as PEM for hydrogen
463 production through electrochemical reforming of aqueous methanol. *Renew Energy* 2016;91:75–
464 82. doi:10.1016/j.renene.2016.01.042.
- 465 29. Uhm S, Jeon H, Kim TJ, Lee J. Clean hydrogen production from methanol-water solutions via
466 power-saved electrolytic reforming process. *J Power Sources* 2012;198:218–22.
467 doi:10.1016/j.jpowsour.2011.09.083.
- 468 30. Hu Z, Wu M, Wei Z, Song S, Shen PK. Pt-WC/C as a cathode electrocatalyst for hydrogen
469 production by methanol electrolysis. *J Power Sources* 2007;166:458–61.
470 doi:10.1016/j.jpowsour.2007.01.083.

- 471 31. Tuomi S, Santasalo-Aarnio A, Kanninen P, Kallio T. Hydrogen production by methanol-water
472 solution electrolysis with an alkaline membrane cell. *J Power Sources* 2013;229:32–5.
473 doi:10.1016/j.jpowsour.2012.11.131.
- 474 32. Caravaca A, De Lucas-Consuegra A, Calcerrada AB, Lobato J, Valverde JL, Dorado F. From
475 biomass to pure hydrogen: Electrochemical reforming of bio-ethanol in a PEM electrolyser. *Appl*
476 *Catal B Environ* 2013;134–135:302–9. doi:10.1016/j.apcatb.2013.01.033.
- 477 33. Caravaca A, Sapountzi FM, De Lucas-Consuegra A, Molina-Mora C, Dorado F, Valverde JL.
478 Electrochemical reforming of ethanol-water solutions for pure H₂ production in a PEM
479 electrolysis cell. *Int J Hydrogen Energy* 2012;37. doi:10.1016/j.ijhydene.2012.03.062.
- 480 34. Jablonski A, Lewera A. Electrocatalytic oxidation of ethanol on Pt, Pt-Ru and Pt-Sn nanoparticles
481 in polymer electrolyte membrane fuel cell-Role of oxygen permeation. *Appl Catal B Environ*
482 2012;115–116:25–30. doi:10.1016/j.apcatb.2011.12.021.
- 483 35. Lamy C, Jaubert T, Baranton S, Coutanceau C. Clean hydrogen generation through the
484 electrocatalytic oxidation of ethanol in a Proton Exchange Membrane Electrolysis Cell (PEMEC):
485 Effect of the nature and structure of the catalytic anode. *J Power Sources* 2014;245:927–36.
486 doi:10.1016/j.jpowsour.2013.07.028.
- 487 36. De Lucas-Consuegra A, De La Osa AR, Calcerrada AB, Linares JJ, Horwat D. A novel sputtered
488 Pd mesh architecture as an advanced electrocatalyst for highly efficient hydrogen production. *J*
489 *Power Sources* 2016;321:248–56. doi:10.1016/j.jpowsour.2016.05.004.
- 490 37. Chen YX, Lavacchi A, Miller H, Bevilacqua M, Filippi J, Innocenti M, Marchionni A,
491 Oberhauser W, Wang L, Vizza F. Nanotechnology makes biomass electrolysis more energy
492 efficient than water electrolysis. *Nat Commun* 2014;5:4036. doi:10.1038/ncomms5036.
- 493 38. Pushkareva IV, Pushkareva AS, Grigorieva SA, Lyutikova EK, Akel'kina SV, Osina MA,
494 Slavcheva EP, Fateev VN. Electrochemical Conversion of Aqueous Ethanol Solution in an
495 Electrolyzer with a Solid Polymer Electrolyte. *Russ J Appl Chem* 2016; 89 :2109–2111. doi:
496 10.1134/S1070427216120260
- 497 39. Lamy C, Devadas A, Simoes M, Coutanceau C. Clean hydrogen generation through the
498 electrocatalytic oxidation of formic acid in a Proton Exchange Membrane Electrolysis Cell
499 (PEMEC). *Electrochim Acta* 2012;60:112–20. doi:10.1016/j.electacta.2011.11.006.
- 500 40. Marshall AT, Haverkamp RG. Production of hydrogen by the electrochemical reforming of
501 glycerol-water solutions in a PEM electrolysis cell. *Int J Hydrogen Energy* 2008;33:4649–54.
502 doi:10.1016/j.ijhydene.2008.05.029.
- 503 41. De Paula J, Nascimento D, Linares JJ. Electrochemical reforming of glycerol in alkaline PBI-
504 based PEM reactor for hydrogen production. *Chem Eng Trans* 2014;41:205–10.
505 doi:10.3303/CET1441035.
- 506 42. de Paula J, Nascimento D, Linares JJ. Influence of the anolyte feed conditions on the performance
507 of an alkaline glycerol electroreforming reactor. *J Appl Electrochem* 2015;45:689–700.
508 doi:10.1007/s10800-015-0848-6.
- 509 43. Jonzalez-Cobos J. Baranton S. Coutanceau C. Development of Bismuth-modified PtPd

- 510 nanocatalysts for the electrochemical reforming of polyols into hydrogen and value-added
511 chemicals. *ChemElectroChem* 2016;3:1694–704.
- 512 44. Sapountzi FM, Tsampas MN, Fredriksson HOA, Gracia JM, Niemantsverdriet JW, Hydrogen
513 from electrochemical reforming of C1-C3 alcohols using proton conducting membranes. *Int J*
514 *Hydrogen Energy*, 2017; 42: 10762-10774, doi: 10.1016/j.ijhydene.2017.02.195
- 515 45. De Lucas-Consuegra A, Calcerrada AB, De La Osa AR, Valverde JL. Electrochemical reforming
516 of ethylene glycol. Influence of the operation parameters, simulation and its optimization. *Fuel*
517 *Process Technol* 2014;127:13–9. doi:10.1016/j.fuproc.2014.06.010.
- 518 46. Miller, H.A.; Bellini, M.; Vizza, F.; Hasenohrl, C.; Tilley RD. Carbon supported Au–Pd core–
519 shell nanoparticles for hydrogen production by alcohol electroreforming. *Catal Sci Technol*
520 2016;6:6870–8.
- 521 47. Liu W, Cui Y, Du X, Zhang Z, Chao Z, Deng Y. High efficiency hydrogen evolution from native
522 biomass electrolysis. *Energy Environ Sci* 2016; 9, 467-472, doi: 10.1039/c5ee03019f
- 523 48. Pagliaro MV, Bellini M, Bevilacqua M, Filippi J, Folliero MG, Marchionni A, Miller HA,
524 Oberhauser W, Caporali S, Innocenti M, Vizza F, *RSC Adv* 2017;7: 13971-13978, doi:
525 10.1039/C7RA00044H
- 526 49. Guenot B, Cretin M, Lamy C, Electrochemical reforming of diethoxymethane in a Proton
527 Exchange Membrane Electrolysis Cell: A way to generate clean hydrogen for low temperature
528 fuel cells. *Int J Hydrogen Energy* 2017: 42: 28128-28139, doi: 10.1016/j.ijhydene.2017.09.028
- 529 50. Liu L, Atomic Layer Deposition of Electrocatalysts for Use in Fuel Cells and Electrolyzers In:
530 Bachmann J, editor. *Atomic Layer Deposition in Energy Conversion Applications 2017*, Wiley-
531 VCH Verlag GmbH&Co KGaA, Weinheim, Germany, 2017, doi: 10.1002/9783527694822.ch5
- 532 51. Mackus AJM, Weber MJ, Thissen NFW, Garcia-Alonso D, Vervuurt RHJ, Assali S, Bol AA,
533 Verheijen MA, Kessels WMM. Atomic layer deposition of Pd and Pt nanoparticles for catalysis:
534 on the mechanisms of nanoparticle formation, *Nanotechnology* 2016;27:034001. doi:
535 10.1088/0957-4484/27/3/034001
- 536 52. Hajara Y, Di Palma V, Kyriakou V, Verheijen MA, Baranova EA, Vernoux P, Kessels WMM,
537 Creatore M, van de Sanden MCM, Tsampas MN. Atomic layer deposition of highly dispersed Pt
538 nanoparticles on a high surface area electrode backbone for electrochemical promotion of
539 catalysis. *Electrochem Commun* 2017;84:40-44. doi: 10.1016/j.elecom.2017.09.023
- 540 53. Penchev H, Borisov G, Petkucheva E, Ublekov F, Sinigersky V, Radev I, Slavcheva E; Highly
541 KOH doped para-polybenzimidazole anion exchange membrane and its performance in Pt/Ti_nO_{2n-1}
542 catalyzed water electrolysis cell. *Materials Letters* 2018; 221: 128-130, doi:
543 10.1016/j.matlet.2018.03.094
- 544 54. Stoll T, Zafeiropoulos G, Tsampas MN. Solar fuel production in a novel polymeric electrolyte
545 membrane photoelectrochemical (PEM-PEC) cell with a web of titania nanotube arrays as
546 photoanode and gaseous reactants. *Int J Hydrogen Energy* 2016;41:17807–17,
547 doi:10.1016/j.ijhydene.2016.07.230
- 548 55. Knoops HCM, Mackus AJM, Donder ME, van de Sanden MCM, Notten PHL, Kessels WMM.

- 549 ALD of platinum and platinum oxide films. *Electrochem Solid-State Lett* 2009;12: G34–G36.
- 550 56. Niemantsverdriet JW, *Spectroscopy in Catalysis*, 3rd Edition, Wiley-VCH, Weinheim; 2007. doi:
551 10.1002/9783527611348
- 552 57. Barradas NP, Jeynes C. Advanced physics and algorithms in the IBA DataFurnace. *Nucl Instrum*
553 *Phys Res B* 2008; 266: 1875-1879, doi: 10.1016/j.nimb.2007.10.044
- 554 58. Hsueh YC, Wang CC, Kei CC, Lin YH, Liu C, Perng TP. Fabrication of catalyst by atomic layer
555 deposition for high specific power density proton exchange membrane fuel cells. *J Catal*
556 2012;294:63-68. doi:10.1016/j.jcat.2012.07.006
- 557 59. Zeng K, Zhang D. Recent progress in alkaline water electrolysis for hydrogen production and
558 applications. *Prog Energy Combust Sci* 2010; 36: 307–326. doi: 10.1016/j.pecs.2009.11.002
- 559 60. Modibedi RM, Ozoemen KI, Mathe MK. Palladium-based nanocatalysts for alcohol
560 electrooxidation in alkaline media. In: Shao M, editor. *Electrocatal. fuel cells A non- low- Platin.*
561 approach, London: Springer-Verlag; 2013, p. 129–56.
- 562 61. Tripkovic AV, Popovic KD, Grgur BN, Blizanac B, Ross PN, Markovic NM, Methanol
563 electrooxidation on supported Pt and PtRu catalysts in acid and alkaline solutions. *Electrochim*
564 *Acta* 2002; 47(22): 3707-3714
- 565 62. Lai SCS, Kleijn SEF, Ozturk FTZ, van Rees Vellinga VC, Koning J, Rodriguez P, Koper MTM,
566 Effects of electrolyte pH and composition on the ethanol electro-oxidation reaction. *Catal Today*
567 2010; 154: 92–104, doi: 10.1016/j.cattod.2010.01.060
- 568 63. Zeng L, Zhao TS, An L, Zhao G, Yan XH, Physicochemical properties of alkaline doped
569 polybenzimidazole membranes for anion exchange membrane fuel cells. *J Membr Sci* 2015; 439:
570 340–348, doi: 10.1016/j.memsci.2015.06.013
- 571 64. Zarrin H, Jiang G, Lam GYY, Fowler M, Chen Z, High performance porous
572 polybenzimidazole membrane for alkaline fuel cells. *Int J Hydrogen Energy* 2014; 39:18405-
573 18415, doi: 10.1016/j.ijhydene.2014.08.134
- 574 65. Jensen JO, Aili D, Hansen MK, Li Q, Bjerrum NJ, Christensen E, A stability study of alkali
575 doped PBI membranes for alkaline electrolyzer cells. *ECS Transactions* 2014: 64 (3):1175-1184,
576 doi: 10.1149/06403.1175ecst
- 577 66. Gilliam RJ, Graydon JW, Kirk DW, Thorpe SJ, A review of specific conductivities of potassium
578 hydroxide solutions for various concentrations and temperatures. *Int J Hydrogen Energy* 2007;
579 32:359 – 364, doi: 10.1016/j.ijhydene.2006.10.062
- 580 67. Ublekov F, Radev I, Sinigersky V, Natova M, Penchev H. Composite anion conductive
581 membranes based on para-polybenzimidazole and Montmorillonite. *Mater Lett* 2018; 219:131-
582 133. doi: 10.1016/j.matlet.2018.02.082
- 583 68. Calcerrada AB, de la Osa A, Llanos J, Dorado F, de Lucas-Consuegra A. Hydrogen from
584 electrochemical reforming of ethanol assisted by sulfuric acid addition. *Appl Catal B* 2018;
585 231:310-316. doi: 10.1016/j.apcatb.2018.03.028
- 586 69. Cheng N, Shao Y, Liu J, Sun X. Electrocatalysts by atomic layer deposition for fuel cell
587 applications. *Nano Energy* 2016; 29:220-242 doi: 10.1016/j.nanoen.2016.01.016

- 588 70. Hasa B, Vakros J, Katsaounis AD. Effect of TiO₂ on Pt-Ru-based anodes for methanol
589 electroreforming. *Appl. Catal. B.* 2018; 237:811-816. doi:10.1016/j.apcatb.2018.06.055
- 590 71. Lim C, Scott K, Allen RG, Roy S. Direct Methanol Fuel Cells Using Thermally Catalysed Ti
591 Mesh. *J Appl Electrochem* 2004; 34:929-933, doi: 10.1023/B:JACH.0000040497.03256.36
- 592 72. Shao ZG, Lin WF, Christensen PA, Zhang H. Ti mesh anodes prepared by electrochemical
593 deposition for the direct methanol fuel cell. *Int J Hydrogen energy* 2006; 31:1914-1919,
594 doi:10.1016/j.ijhydene.2006.05.003
- 595 73. De Souza RFB, Buzzo GS, Silva JCM, Spinace EV, Neto AO, Assumpcao MHMT. Effect of
596 TiO₂ Content on Ethanol Electrooxidation in Alkaline Media Using Pt Nanoparticles Supported
597 on Physical Mixtures of Carbon and TiO₂ as Electrocatalysts *Electrocatalysis* 2014; 5:213-
598 219. doi:10.1007/s12678-014-0183-4
- 599 74. Yoo SJ, Jeon TY, Lee KS, Park KW, Sung YE. Effects of particle size on surface electronic and
600 electrocatalytic properties of Pt/TiO₂ nanocatalysts. *Chem Commun* 2010; 46:794-796, doi:
601 10.1039/B916335B
- 602 75. Park SB, Park YI, Fabrication of Gas Diffusion Layer (GDL) Containing Microporous Layer
603 Using Flourinated Ethylene Prophylene (FEP) for Proton Exchange Membrane Fuel Cell
604 (PEMFC). *Int J Precis Eng Manuf* 2012; 13: 1145-1151, doi: 10.1007/s12541-012-0152-x
- 605 76. Su H, Sita C, Pasupathi S. The effect of gas diffusion layer PTFE content on the performance of
606 high temperature proton exchange membrane fuel cell. *Int J Electrochem Sci* 2016; 11: 2919 –
607 2926. doi: 10.20964/110402919
- 608

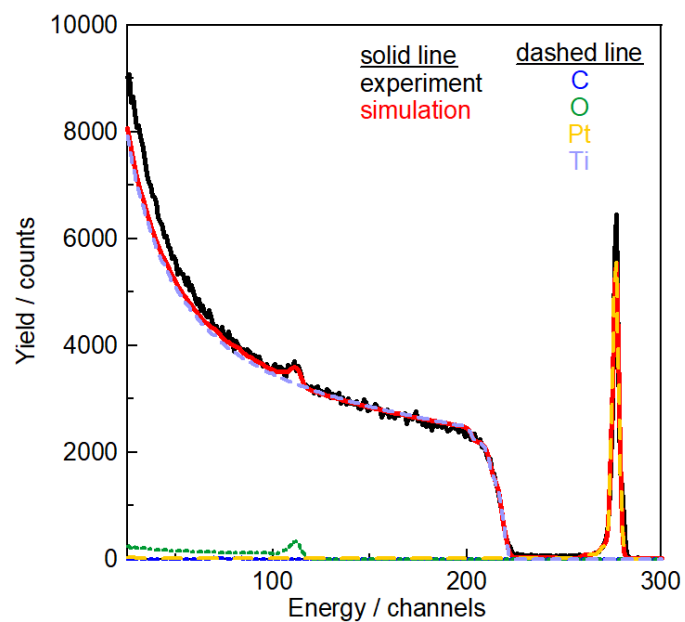


Figure S1. The experimental (solid black line) and simulated (solid red line) RBS spectrum of the Pt/TiO₂-Ti sample. The simulated elemental contributions are over-plotted using dashed lines. The legend indicates the corresponding elements.

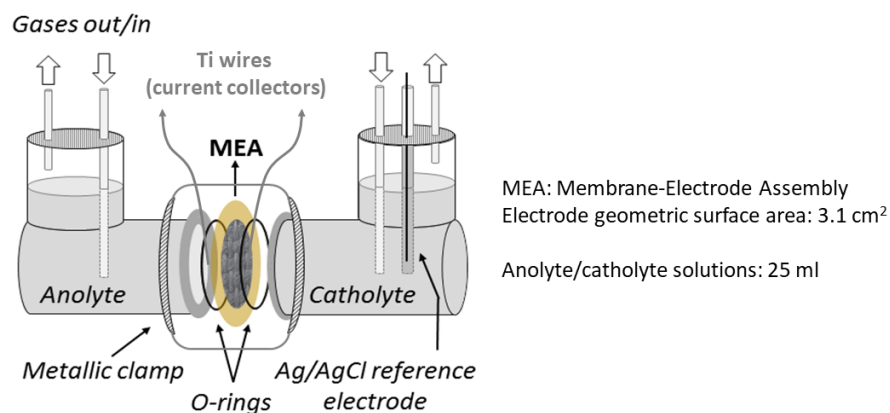


Figure S2. Schematic representation of the electrochemical cell. The two chambers are separated by the MEA and a metallic clamp is used to hold together the assembly. The Ag/AgCl reference is inserted at the cathodic chamber.